The Plant Cell, Vol. 15, 1170–1185, May 2003, www.plantcell.org © 2003 American Society of Plant Biologists

Cloning and Characterization of the *WAX2* Gene of Arabidopsis Involved in Cuticle Membrane and Wax Production

Xinbo Chen, S. Mark Goodwin, Virginia L. Boroff, Xionglun Liu, and Matthew A. Jenks[1]

Department of Horticulture and Landscape Architecture, Purdue University, West Lafayette, Indiana 47907

Insertional mutagenesis of Arabidopsis ecotype C24 was used to identify a novel mutant, designated *wax2*, that had alterations in both cuticle membrane and cuticular waxes. Arabidopsis mutants with altered cuticle membrane have not been reported previously. Compared with the wild type, the cuticle membrane of *wax2* stems weighed 20.2% less, and when viewed using electron microscopy, it was 36.4% thicker, less opaque, and structurally disorganized. The total wax amount on *wax2* leaves and stems was reduced by >78% and showed proportional deficiencies in the aldehydes, alkanes, secondary alcohols, and ketones, with increased acids, primary alcohols, and esters. Besides altered cuticle membranes, *wax2* displayed postgenital fusion between aerial organs (especially in flower buds), reduced fertility under low humidity, increased epidermal permeability, and a reduction in stomatal index on adaxial and abaxial leaf surfaces. Thus, *wax2* reveals a potential role for the cuticle as a suppressor of postgenital fusion and epidermal diffusion and as a mediator of both fertility and the development of epidermal architecture (via effects on stomatal index). The cloned *WAX2* gene (verified by three independent allelic insertion mutants with identical phenotypes) codes for a predicted 632–amino acid integral membrane protein with a molecular mass of 72.3 kD and a theoretical pI of 8.78. WAX2 has six transmembrane domains, a His-rich diiron binding region at the N-terminal region, and a large soluble C-terminal domain. The N-terminal portion of WAX2 is homologous with members of the sterol desaturase family, whereas the C terminus of WAX2 is most similar to members of the short-chain dehydrogenase/reductase family. WAX2 has 32% identity to CER1, a protein required for wax production but not for cuticle membrane production. Based on these analyses, we predict that WAX2 has a metabolic function associated with both cuticle membrane and wax synthesis. These studies provide new insight into the genetics and biochemistry of plant cuticle production and elucidate new associations between the cuticle and diverse aspects of plant development.

INTRODUCTION

The plant cuticle forms the outermost coating over essentially all aerial plant surfaces and provides a protective barrier to many forms of environmental stress, including those caused by drought, phytophagous insects, and pathogens (Eigenbrode and Espelie, 1995; Jenks and Ashworth, 1999; Jenks, 2002). One of the cuticle's most important functions is limiting transpiration to conserve water, a mechanism especially important for plant survival in water-limited environments such as those found in desert, alpine, and coastal ecosystems (Schreiber and Riederer, 1996; Riederer and Schreiber, 2001; Jenks, 2002). As described by Jeffree (1996), the plant cuticle is a complex structure composed of two basic layers: an outermost epicuticular wax layer that overlies a cuticle membrane layer. Epicuticular waxes often are visible to the naked eye as a bluish-white coating called glaucousness or bloom. By scanning electron microscopy, these glaucous waxes are visible as a field of densely distributed wax crystals, with diverse shapes specific to species and organs. Nonglaucous and glossy leaf surfaces have a smooth coating of wax or may possess very sparsely distributed wax crystals. Using transmission electron microscopy, the cuticle membrane in most plants is seen to possess two basic layers: an outer translucent cuticle proper and an inner opaque cuticular layer defined by the presence of osmiophilic cellulose microfibrils (Jeffree, 1996). Compositionally, the epicuticular waxes are primarily long-chain aliphatic molecules that are soluble in organic solvents, whereas the cuticle membrane is composed primarily of insoluble cutin polyester with lesser amounts of intracuticular waxes.

To date, nine genes associated with plant cuticular wax production have been cloned, including five from Arabidopsis. Four of these—*CER2*, *CER3*, *GL2*, and *GL15*—appear to encode regulatory loci (Tacke et al., 1995; Hannoufa et al., 1996; Moose and Sisco, 1996; Negruk et al., 1996; Xia et al., 1996), three—*CER6*, *KCS1*, and *GL8*—may encode metabolic enzymes (Xu et al., 1997; Millar et al., 1999; Todd et al., 1999; Fiebig et al., 2000), and two—*CER1* and *GL1*—may be involved in either the transport or the metabolism of wax compounds (Aarts et al., 1995; Hansen et al., 1997). None of these genes has been associated with cuticle membrane synthesis.

Only two cuticle membrane mutants, sorghum *bm2* and maize *cr4*, have been reported in plants. The *bm2* mutant has >60% reduction in cuticle membrane weight and thickness (Jenks et al., 1994) and a significant alteration in its waxes (Jenks et al., 2000). The *BM2* gene has not been cloned. The *cr4* mutant displays an irregularly thickened cuticle membrane and postgenital fusion, a condition in which organs, after being formed, fuse together upon physical contact (Jin et al., 2000;

[1] To whom correspondence should be addressed. E-mail jenks@hort.purdue.edu; fax 765-494-0391.

Article, publication date, and citation information can be found at www.plantcell.org/cgi/doi/10.1105/tpc.010926.

Becraft et al., 2001). Whether *cr4* affects waxes was not reported. The *CR4* gene was cloned and shown to encode a receptor-like kinase involved in the regulation of global aspects of leaf development rather than strictly cuticle membrane metabolism. Other genes were cloned whose predicted protein sequences suggest functions in the synthesis of cutin (the primary component of cuticle membrane); these genes include *CYP86A1*, *CYP94A1*, *CYP94A2*, and *LCR* (Benveniste et al., 1998; Tijet et al., 1998; LeBouquin et al., 1999; Wellesen et al., 2001). However, these genes have yet to be linked with cutin synthesis in planta.

We recently used insertion mutagenesis to isolate a cuticle membrane mutant in Arabidopsis designated *wax2*. Compared with that of the wild type, the cuticle membrane of *wax2* weighed less, was thicker, was much less reticulated, and was structurally disorganized. Besides altered cuticle membrane, *wax2* had a glossy stem, similar to that of the Arabidopsis epicuticular wax mutants designated *eceriferum* (*cer*). *wax2* also displayed postgenital fusion. Comparable Arabidopsis stem wax mutants displaying postgenital fusion were reported previously, including *wax1* (Jenks et al., 1996), *ded1* (Lolle et al., 1998), and *cer10* and *cer13* (Jenks et al., 2002). Whether these mutants, like *wax2*, have altered cuticle membranes is unknown. *wax2* also had reduced fertility, a condition reported for many *cer* mutants (Koornneef et al., 1989), increased epidermal permeability similar to that of the sorghum cuticle membrane mutant *bm2* (Jenks et al., 1994), and a lower stomatal index. By comparison, the *cer1* and *cer6* wax mutants had higher stomatal indices (Gray et al., 2000). Thus, the *wax2* mutation reveals a unique cuticle gene involved in diverse aspects of plant development. We describe here the cloning and characterization of *WAX2*, a cuticle membrane gene from Arabidopsis.

RESULTS

Isolation and Genetic Analysis of the *wax2* Mutant

Approximately 35,000 families from a T-DNA–mutagenized population of Arabidopsis ecotype C24 (created as described by Weigel et al., 2000) were screened to identify mutants with reduced visible glaucousness of the inflorescence stem. These stem wax mutants then were screened for changes in the rate of water loss from excised stems (Jenks et al., 1994). One mutant (later designated *wax2*) had a higher water-loss rate than the wild type and all other mutants. Gravimetric and transmission electron microscopy studies showed that the *wax2* mutant had dramatic alterations in the cuticle membrane (see below).

The activation T-DNA vector pSKI015 insert used for mutagenesis contains the *BAR* gene for bialophos resistance. Bialophos-resistant plants segregated in an approximate 3:1 (resistant:susceptible) ratio (χ^2 test on 259 plants, $P > 0.05$) in a backcross F2 population, indicating the presence of a single bialophos-active T-DNA insert. Cosegregation of bialophos resistance, the glossy stem, and small, nearly seedless siliques was consistent with the genetic linkage of these phenotypes and the monogenic recessive inheritance of the responsible *wax2* allele. Postgenital fusion of *wax2* segregants in the F2 population showed variable penetrance in the low-humidity environment in which the plants were grown. No glaucous wild-type segregants showed fusion or low fertility. Fifteen randomly selected glossy, reduced fertility segregants had higher excised stem water loss rates than 15 wild-type segregants, indicating cosegregation of high transpiration and the visible mutant phenotypes. Gel blot analysis of DNA from *wax2* digested with the restriction enzymes BamHI, EcoRI, and HindIII using the *BAR* gene probe revealed the presence of only one hybridizing band (data not shown), providing further evidence that a single insertion in the *WAX2* gene was responsible for the described phenotypes.

Cuticle Membrane Alteration

Wild-type stem cuticles have a typical type-3 cuticle structure (Jeffree, 1996), with an amorphous cuticle proper and a reticulate cuticular layer (visualized by transmission electron microscopy). The cuticle ultrastructure of *wax2* stems was altered dramatically compared with that of wild-type stems (Figure 1). The cuticle membrane thickness of *wax2* stems was increased by 36.4% relative to that of the wild-type (cuticle proper plus cuticular layer). *wax2* cuticle membranes were 151.7 nm thick, whereas wild-type membranes were 111.2 nm thick. The osmiophilic reticulum typical of the cuticular layer of wild-type membranes, and the normally visible line of demarcation between the cuticle proper and the cuticular layer, were nearly absent in *wax2* membranes. The connective region between the cuticle membrane and the cell wall was irregular and disorganized in *wax2*, showing distinct, unorganized bulges of less reticulate or nonreticulate cuticle extending into outer cell wall regions. The outer epidermal cell wall of *wax2* was more darkly stained (osmiophilic) than that of the wild type (Figure 1). Interestingly, $ZnCl_2$-extracted cuticle membranes of *wax2* stems had 20.2% less total weight than those of wild-type stems, even though *wax2* cuticles were thicker. Stem cuticle membrane weight was reduced from 11.9 mg/dm^2 in the wild type to 9.5 mg/dm^2 in *wax2*. The stem cuticle membrane weight and ultrastructure of five *cer* mutants, including *cer1*, were not significantly different from those of the wild type (data not shown). Likewise, *wax2* leaf cuticle membranes were thicker than those in the wild type (data not shown).

Cuticular Wax Alteration

Scanning electron microscopy was used to show that the density of wax crystals on the *wax2* stem was reduced severely (to nearly no wax crystals in places) relative to the wild type (Figure 2). Where present in *wax2*, there was a higher proportion of horizontal plate–like wax crystals and corresponding reductions in vertical plate–like and upright tubular wax crystals. Leaf surfaces of C24 and *wax2* lack visible wax crystals (data not shown). Relative to the wild type, total stem and leaf wax on *wax2* were reduced by 78.3 and 80.3%, respectively (Table 1). The wax composition on *wax2* stems was characterized as having large proportional reductions in aldehydes, alkanes, secondary alcohols, and ketones, with corresponding increases in acids, primary alcohols, and esters (Table 1). The *wax2* mutation produced a slightly different effect on leaf than stem waxes

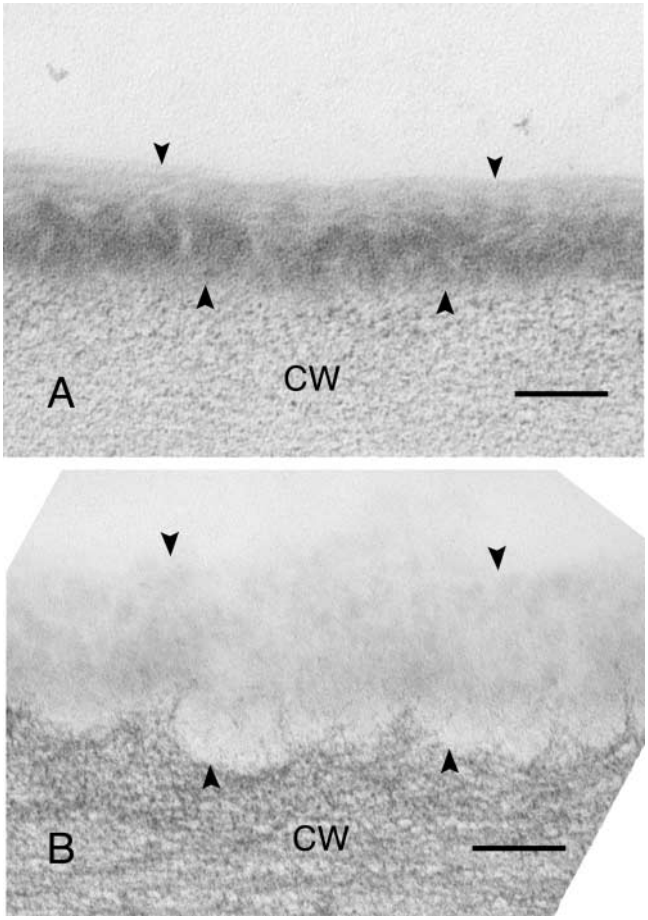

Figure 1. Arabidopsis Ecotype C24 and *wax2* Mutant Stem Pavement Cell Cuticle Membranes Visualized Using Transmission Electron Microscopy.

(A) The stem cuticle membrane (between arrowheads) on wild-type C24 is clearly divided into an outermost, more electron-translucent cuticle proper and an innermost, more opaque reticulated cuticular layer. CW, cell wall. Bar = 100 nm.

(B) The stem cuticle membrane (between arrowheads) on *wax2* is thicker and does not show the typical bilayer ultrastructure, lacking the dark-staining reticulum normally associated with the cuticular layer. The more translucent cuticle material bulges into the outer cell wall layer, revealing a disruption of the normal cutinization process. The outer cell walls of *wax2* are more darkly stained relative to wild-type cell walls, indicating the accumulation of new osmiophilic materials in *wax2*. CW, cell wall. Bar = 100 nm.

in that only the alkane proportions were reduced on leaves of *wax2* (Table 1). Total proportions of acids, primary alcohols, and esters were increased greatly on *wax2* leaves relative to wild-type leaves, with *wax2* leaf aldehyde proportions increased just slightly (Table 1). Secondary alcohols and ketones are trace constituents on leaves of both the wild type and *wax2* and are not discussed further. For individual wax constituents, the absolute amount of C_{30} primary alcohols on *wax2* stems was ~180% greater than on wild-type stems, whereas the amounts of all other *wax2* stem constituents were reduced relative to those of the wild type (Figure 3). The increased C_{30} alcohols on *wax2* stems are consistent with shunting of the C_{30} acyl-CoA precursors (normally converted primarily to C_{29} alkanes) toward the primary alcohol branch of the wax pathway. The leaves of *wax2* did not exhibit a similar skewing in the chain length distribution of wax homologs, except that certain shorter chain length wax constituents in all classes were reduced less (or increased slightly) than longer chain waxes compared with the wild type (Figure 3). This differential effect on short-chain versus long-chain leaf waxes was small.

Molecular Cloning of the *WAX2* Gene

Plant DNA fragments of 1.4 and 1.1 kb flanking the T-DNA insert were rescued from the *wax2* right border by EcoRI and HindIII, respectively. Sequencing results indicated that they represented the same insert site. A PCR assay showed that 25 randomly selected mutants in a backcross F2 population were homozygous for the T-DNA insert, indicating tight linkage between the insert and the visible *wax2* mutant phenotypes. The insert occurred in the third intron of a putative Arabidopsis *GLOSSY1* homolog, At5g57800. The gene At5g57800 was predicted to generate an mRNA transcript of 1917 bp, which encoded a 566–amino acid protein with similarity to the predicted GL1, CER1, and CER1-like proteins but ~70 amino acids shorter at the N terminus.

To be certain that we had obtained the full-length *WAX2* mRNA sequence, we performed 5′ and 3′ rapid amplification of cDNA ends (RACE) using gene-specific primers designed from EST sequences available at the Arabidopsis EST stock center. A 1759-bp 5′ RACE fragment and a 1259-bp 3′ RACE fragment were obtained with 498 bp overlap of 100% sequence match. Both sequences aligned to the genomic DNA and ESTs. Compared with the At5g57800 sequence, our 5′ RACE fragment of *WAX2* contained an additional exon (17,352 to 17,402 bp of MTI20) upstream of the original first exon. As such, the T-DNA insert occurs in the fourth intron of *WAX2*. The full *WAX2* nucleotide sequence and associated annotation are available in GenBank. The full-length *WAX2* spans 3813 bp of genomic DNA and has 11 exons and 10 introns. Exons range from 51 to 257 bp, and introns range from 75 to 313 bp. The full-length cDNA is 2500 bp and has a coding region of 1899 bp, a 376-bp 5′ untranslated region, and a 193-bp 3′ untranslated region. The 5′ untranslated region contains five contiguous stop codons immediately before the start codon, and there are no other alternative start codons within it. A TATA box (TATATAAG) at position −35 bp and two CAAT boxes at −7 and −289 bp relative to the 5′ end of the transcription start site are present. The 3′ untranslated region possesses a putative polyadenylation signal (AAAAA).

After cloning and characterization of the WAX2 sequence, a second *wax2* allelic mutant in the Columbia ecotype with a T-DNA insert in the third exon (SAIL 832 E06), designated *wax2-2*, was obtained from Syngenta (Basel, Switzerland). A third *wax2* allelic mutant in the Columbia ecotype with a T-DNA insert in the fifth exon, obtained from the Salk Institute through the ABRC Stock Center (SALK 034318) and designated *wax2-3*, was identified in the Salk T-DNA–tagged lines. The SALK 034318 insertion mutant information was obtained from the SIGnAL World Wide

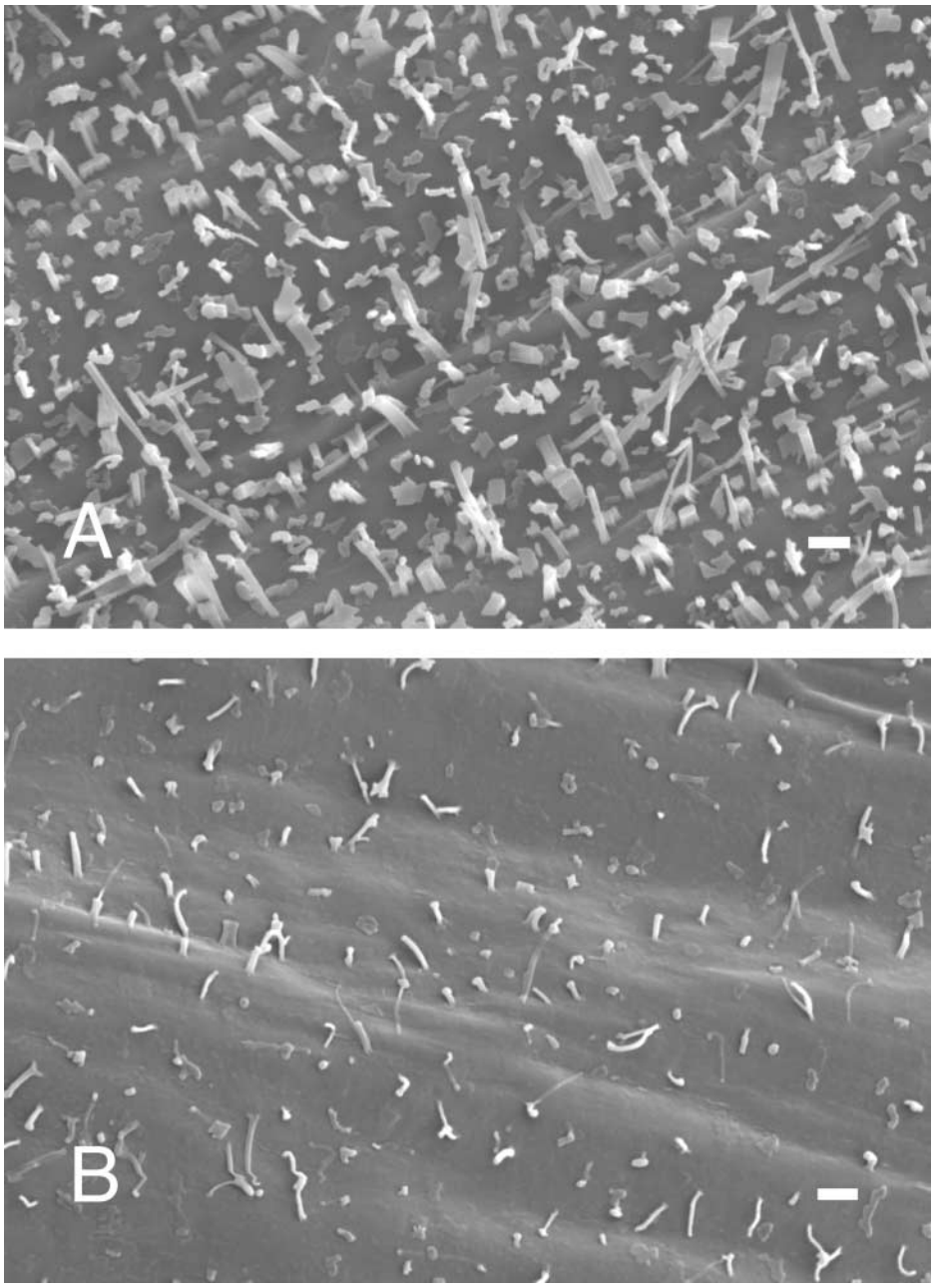

Figure 2. Epicuticular Wax Crystallization Patterns on Stem Surfaces of Arabidopsis Ecotype C24 and the *wax2* Mutant Visualized Using Scanning Electron Microscopy.

(A) Wax crystals on stems of wild-type C24 are very dense, with a high proportion of vertical plate–like and tubular wax crystals. Bar = 5 μm.
(B) Wax crystals on stems of *wax2* are much reduced in density relative to the wild type and possess a higher proportion of horizontal plate–like wax crystals. Bar = 5 μm.

Web site (http://signal.salk.edu). Both *wax2-2* and *wax2-3* displayed the same visible glossy stem, reduced fertility, and postgenital fusions as the original *wax2-1* mutant. PCR genotyping of *wax2-2* and *wax2-3* in a backcross F2 population indicated that all mutants were homozygous for the insert *wax2* sequence. In addition, *wax2-2* and *wax2-3* phenotypic segregation ratios in F2 populations showed monogenic recessive inheritance, as did *wax2-1*. These data confirm that the independent insertions in the *WAX2* sequence are responsible for the altered visible phenotypes of these mutants. The *wax2* mutant complemented *wax1* in a test of allelism, and *WAX2* was not closer than an estimated 20 centimorgan to any of the existing *cer* loci on chromosome 5 (A.M. Rashotte, M.A. Jenks, and K.A. Feldmann, unpublished data).

Table 1. Stem and Leaf Cuticular Waxes on Wild-Type Arabidopsis Ecotype C24 and the Isogenic *wax2* Mutant

		Stem		Leaf	
Wax	Measurement	C24	*wax2*	C24	*wax2*
Acid	Amount	47.9 ± 16.8	17.8 ± 14.3	8.2 ± 0.4	4.8 ± 0.8
	Percentage	1.6 ± 0.4	2.6 ± 1.9	8.0 ± 0.7	24.9 ± 9.3
Aldehyde	Amount	120.3 ± 25.4	18.3 ± 1.2	4.9 ± 0.6	1.9 ± 0.4
	Percentage	4.0 ± 0.4	2.8 ± 0.1	4.8 ± 0.9	9.4 ± 3.6
1-Alcohol	Amount	334.5 ± 23.7	324.2 ± 28.7	13.4 ± 2.8	8.0 ± 3.4
	Percentage	11.3 ± 0.7	50.1 ± 0.7	12.9 ± 1.7	37.9 ± 9.9
Alkane	Amount	1578.1 ± 171.1	132.3 ± 4.0	75.0 ± 13.1	1.8 ± 0.8
	Percentage	52.9 ± 0.9	20.6 ± 2.3	72.1 ± 2.9	8.3 ± 3.4
2-Alcohol	Amount	137.4 ± 37.3	16.2 ± 6.4	Trace	Trace
	Percentage	4.6 ± 0.9	2.5 ± 0.9	Trace	Trace
Ketone	Amount	679.5 ± 39.4	71.5 ± 18.9	Trace	Trace
	Percentage	22.9 ± 1.2	11.0 ± 2.4	Trace	Trace
Ester	Amount	81.9 ± 12.8	67.4 ± 8.9	2.3 ± 0.4	4.0 ± 1.6
	Percentage	2.8 ± 0.6	10.4 ± 1.0	2.2 ± 0.3	19.5 ± 6.1
Total	Amount	2979.6 ± 288.8	647.7 ± 56.7	103.8 ± 15.6	20.5 ± 3.8

Mean total wax amount (μg/dm ± SD), total amount of each wax class (μg/dm ± SD), and percentage of each class within each sample extract are shown. 1-Alcohol and 2-alcohol, primary and secondary alcohol, respectively.

Characterization of the Predicted WAX2 Protein

The *WAX2* transcript encodes a polypeptide of 632 amino acids with an estimated molecular mass of 72.3 kD and a theoretical pI of 8.78. No alternative open reading frames were identified. WAX2 protein had highest sequence similarities to a partial *Senecio odora* cDNA clone named *epi23* (Hansen et al., 1997) and a partial rice sequence annotated as a GLOSSY1 homolog (Hansen et al., 1997), with 65 and 63% amino acid identity, respectively (Figure 4). WAX2 has 35% amino acid identity to GLOSSY1 in maize (Hansen et al., 1997) and 34% amino acid identity to CER1 in Arabidopsis (Aarts et al., 1995). WAX2 amino acid identity to three other CER1-like paralogs in Arabidopsis varied between 31 and 34%. The C-terminal sequences of the WAX2 polypeptide (366 to 553 amino acids) and its rice and *Senecio* homologs were highly similar (83 and 80% identity, respectively, to WAX2), suggesting that this region may have similar functions in all three species. Similar to the CER1 and CER1-like proteins, WAX2 appears to be an integral membrane protein possessing highly conserved transmembrane-spanning domains at its N terminus. Specifically, WAX2 is predicted to have six transmembrane-spanning domains between residues 42 and 64, 95 and 117, 127 and 146, 186 and 208, 301 and 323, and 330 and 349 of the deduced WAX2 protein (TMHMM Program; data not shown). The N-terminal end of WAX2 (including the transmembrane domain) was 95.4% aligned to the signature sequence (coding domain [CD] length of 216 residues) of the sterol desaturase family.

The WAX2 protein also was found to possess the three His-rich motifs (HX3H, HX2HH, and HX2HH, where X stands for any amino acid) of the SUR2-type hydroxylase/desaturase catalytic domains (Figure 4). Based on TMHMM Program analysis, the C terminus (residues 350 to 632) is located outside of a membrane. A span of 66 amino acids (residues 456 to 521) near the C-terminal end shares 33% identity and 49% similarity to a domain found in retinol dehydrogenase. Residues 456 to 497 were 16.7% aligned to a signature (CD length of 252 residues) found in the short-chain dehydrogenase/reductase family (SDR). Computer-based homology searches using various BLAST (Basic Local Alignment Search Tool) and FASTA algorithms with phylogenetic analysis revealed that the *Senecio* EPI23 and Rice GL1 sequences are more appropriately termed WAX2 homologs (Figure 5). The WAX2 homologs and GL1 form a distinct group separate from CER1, CER1L19 (Figure 5), and two other CER1-like proteins (data not shown) in Arabidopsis.

Analysis of *WAX2* Transcript Expression

The 5′ RACE *WAX2* cDNA fragment was used as a probe in RNA gel blot experiments. After plants bolted, total RNA was isolated from different organs of wild-type and *wax2* mutant plants. These studies revealed a 2.5-kb mRNA band in stems, rosette leaves, siliques, and whole flowers of the wild type (Figure 6). The amount of *WAX2* transcripts was highest in siliques and lower in leaves than in stems and flowers. The *WAX2* transcript was not detected in root RNA of the wild type. These results are similar to those reported for *CER1* RNA expression (Aarts et al., 1995), except that the highest expression of *WAX2* occurred in siliques, whereas the highest expression of *CER1* occurred in flowers. The RNA isolated from *wax2-1*, *wax2-2*, and *wax2-3* lacked the *WAX2* transcript in all organs examined (data not shown). The lack of transcript and the location of the insert suggest that all three *wax2* insertional alleles are functional knockouts.

Pleiotropic Effects of *wax2*

Postgenital fusions between aerial organs in the *wax2* mutant were common (Figure 7), although the penetrance and expressivity of this trait in *wax2* populations was variable, occurring

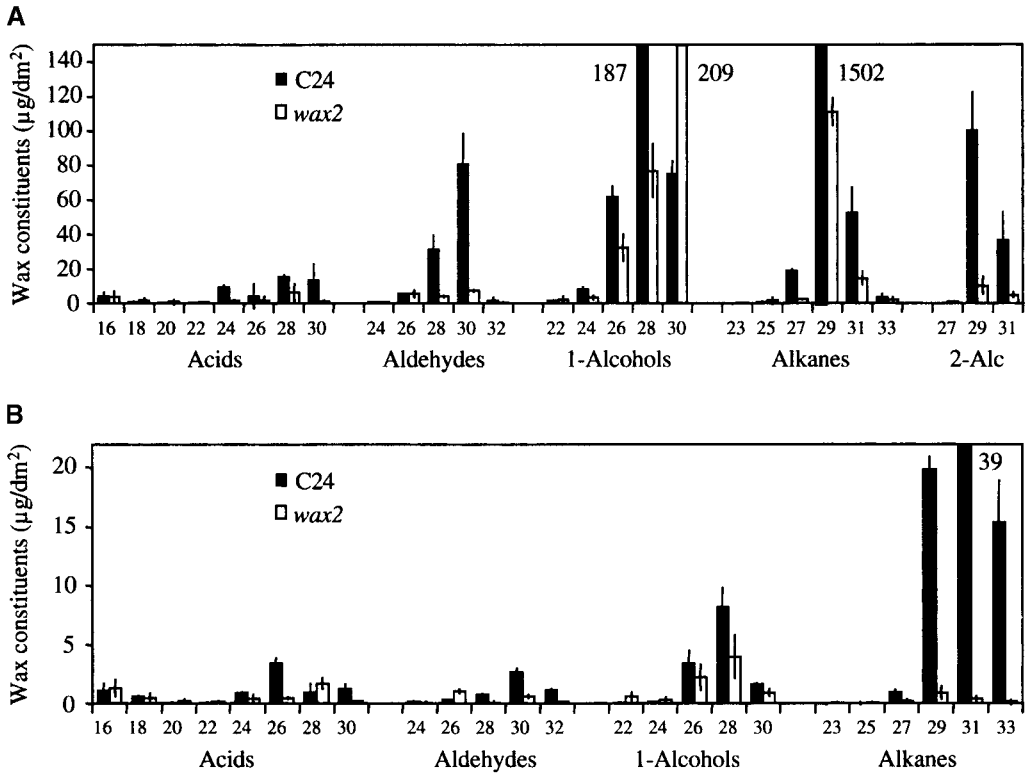

Figure 3. Stem Cuticular Wax Constituents on Arabidopsis Ecotype C24 and the *wax2* Mutant.

(A) Inflorescence stems.

(B) Leaf blades.

Chain lengths are labeled on the horizontal axis. Where the cuticular wax constituent amount was off the scale, a number designating the actual value is shown next to the bar. Ketones were all 29 carbons, and ester chain lengths were not determined. Secondary alcohols (2-Alc) and ketones were only trace constituents in leaf waxes (see Table 1 for total quantities in each class).

with greater frequency in the greenhouse than in growth rooms. Fusions were seen to occur between many aerial organs, especially between leaves, sepals (i.e., flower buds), sepals and leaves, leaves and stems, and sepals and stems. Gently clamping together fully expanded *wax2* leaves did not produce fusions, suggesting that the competence for fusion occurs in primordial or young expanding organs but not in older organs. Fusion between two or more *wax2* plants growing in close contact was not observed. In addition, the penetrance of the fusion phenotype was never 100%.

wax2 showed a significant reduction in fertility in a low-humidity atmosphere under open pollination, as revealed by very small siliques (Figure 7) with very few (if any) seeds produced relative to the wild type. Plants open pollinated in high-humidity conditions showed restored fertility. To determine whether *wax2* sterility was male or female specific, reciprocal crosses were made by hand between *wax2* and the isogenic wild type. Under low-humidity conditions (~30% RH, and without bagging after crossing), 78.1% of siliques (25 of 32) produced seeds in crosses made using *wax2* as the female and the wild type as the male pollen donor (*wax2/WAX2*) and 76.2% of siliques (16 of 21) produced seeds in the *WAX2/WAX2* cross. In the *WAX2/wax2* and *wax2/wax2* crosses, 0 of 29 and 0 of 21 siliques produced seeds, respectively. Under high-humidity conditions (bagging after crossing), 78.3% of siliques (18 of 23) produced seeds in the *wax2/WAX2* cross, 70.8% (17 of 24) produced seeds in the *WAX2/wax2* cross, 80.9% (17 of 21) produced seeds in the *WAX2/WAX2* cross, and 66.7% (14 of 21) produced seeds in the *wax2/wax2* cross. As with *cer1* (Aarts et al., 1995) and *cer6-2* (Preuss et al., 1993), sterility appeared limited to the male reproductive system and was dependent on humidity.

Adaxial and abaxial leaves of *wax2* had a 16.0 and 17.4% lower stomatal index than wild-type leaves (Table 2). Whereas wild-type C24 leaves had an adaxial stomatal index of 29.4 ± 0.74 and an abaxial stomatal index of 29.3 ± 0.3, *wax2* leaves had an adaxial stomatal index of 24.7 ± 0.5 and an abaxial stomatal index of 24.2 ± 0.9. The size and general morphology of *wax2* stomata appeared normal, although electron microscopy studies are needed to verify this finding. The stomatal and pavement cell density was higher in *wax2* than in the wild type (Table 2). *wax2* leaves were slightly smaller than wild-type leaves, indicating that there was probably less expansion of epidermal cells in *wax2* than in the wild type during leaf development.

Chlorophyll efflux studies showed that rates of chlorophyll extraction by 80% ethanol during a 24-h period were greater in

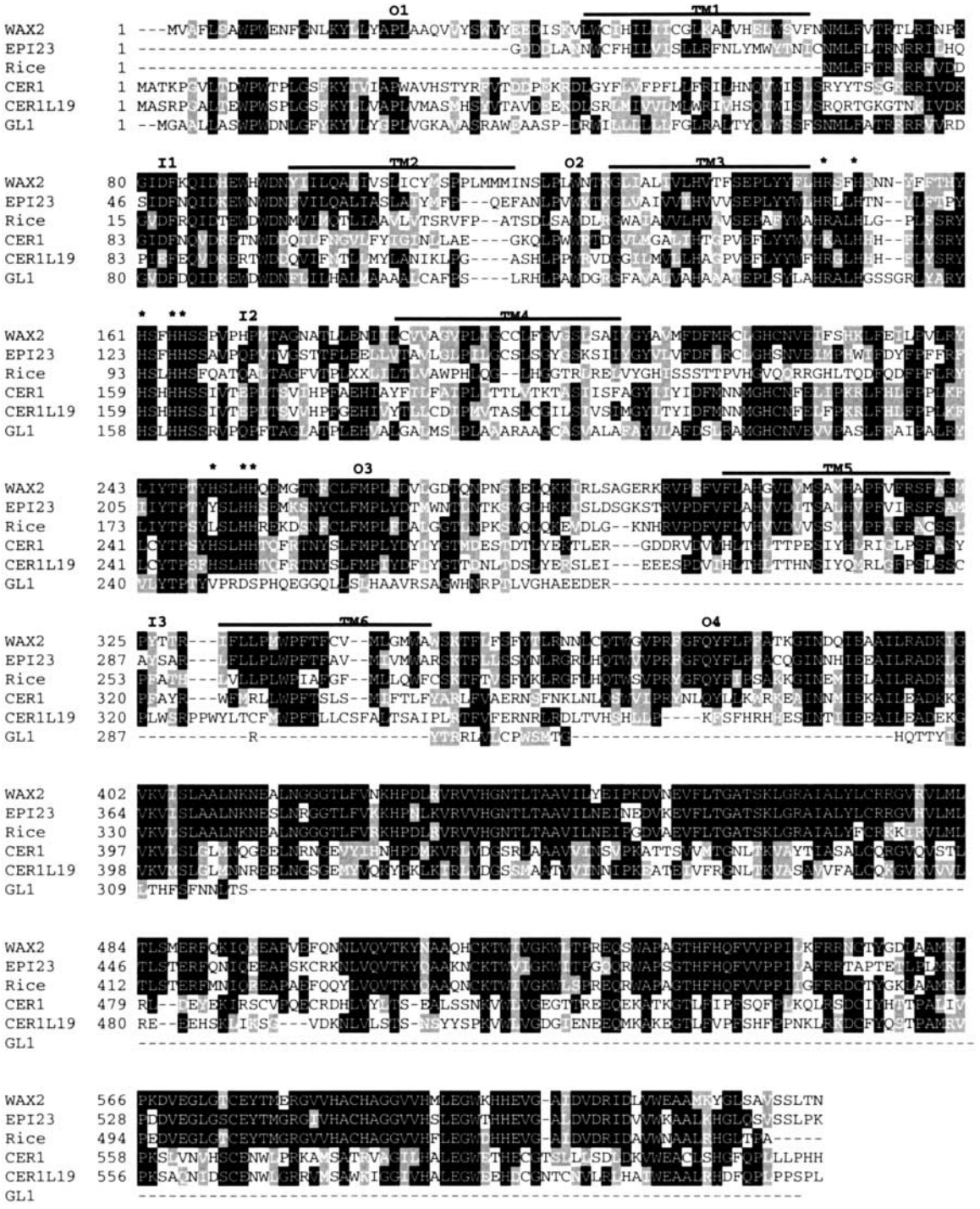

Figure 4. Alignment of Arabidopsis WAX2 with Five Related Proteins.

The alignment consists of the following predicted protein sequences: *Senecio odorus* partial protein sequence (EPI23), rice GLOSSY1 homolog fragment, Arabidopsis CER1, Arabidopsis CER1L19, and maize GLOSSY1 (GL1). Sequences were aligned with CLUSTAL W using default parameters. Identical and similar residues are shown on black and gray backgrounds, respectively. Gaps required for optimal alignment are indicated by dashes. Putative transmembrane domains (TM1 to TM6) of WAX2, determined with the TMHMM program, are indicated by lines above the sequences, and outer (O1 to O4) and inner (I1 to I3) membrane segments also are indicated. The eight conserved His residues in the three His-rich motifs of the sterol desaturase family are marked above the alignment with stars.

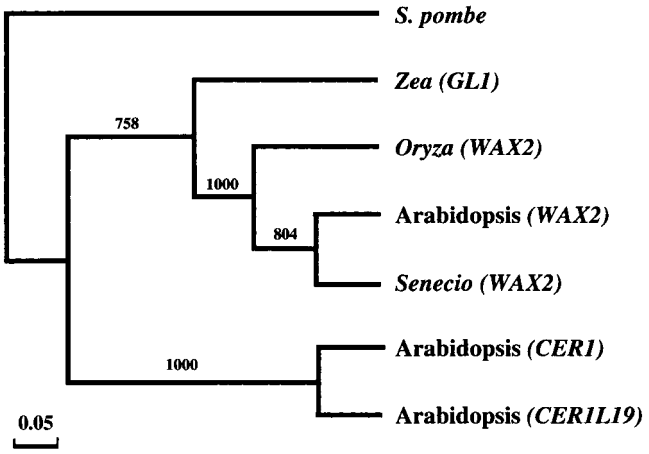

Figure 5. Phylogenetic Analysis of WAX2.

Phylogram derived from a data set of deduced polypeptides for Arabidopsis WAX2 and related deduced polypeptides. The rooted tree was constructed using CLUSTAL W (Thompson et al., 1994). The data set consisted of the six polypeptides shown in Figure 4 and a yeast C-4 methyl sterol oxidase of the desaturase family (*S. pombe*). Numerals above the lines represent bootstrap percentages (based on 100 replicates).

both leaves and stems of *wax2* than in the wild type (Figure 8). In addition, preflowering *wax2* rosettes sustained greater foliar injury than wild-type rosettes when sprayed with either acifluorfen or paraquat. Visual scoring using a modified Horsfall-Barret scale revealed 81% discoloration and 80% wilting of *wax2* leaves compared with 21% discoloration and 27% wilting of wild-type leaves at 24 h after paraquat application. Results using acifluorfen were similar (data not shown). In addition, epidermal permeability to water vapor was higher in *wax2* than in the wild type and all other mutants examined (Figure 9). *wax2* plants had higher transpiration rates than wild-type plants in both light and dark environments but had normal stomatal closure response time after transfer from light to darkness and normal stomatal opening response time after transfer from dark to light (Figure 9). Similar results were seen for whole preflowering plants (data not shown).

DISCUSSION

The WAX2 Protein Functions in Cuticle Membrane and Wax Production

The *wax2* mutant's reduction in cuticle membrane reticulation and the presence of regular bulges of cuticular material in outer cell walls indicate that the *wax2* cuticle membrane undergoes very irregular development. Increased thickness and increased translucence, along with the loss of general organization of the *wax2* cuticle membrane, suggest a potential disruption in the linkages that normally hold the cuticle membrane lipids together. Whether these changes are caused by alterations in the synthesis of certain cutin monomers (the major cuticle membrane subunit) or by covalent bonds between cutin monomers that form the cutin polyester framework of the membrane remains unclear.

Previous studies suggest that wax compositional changes such as those that occur in *wax2* could not have caused these ultrastructural changes in *wax2* cuticle membrane. First, exhaustive extraction of waxes from cuticles does not alter cuticle membrane ultrastructure, except for a slight reduction in the visibility of cuticle proper lamellae (Viougeas et al., 1995). Second, the cuticle membranes of seven wax mutants in sorghum and five wax mutants in Arabidopsis, including *cer1*, were ultrastructurally normal (Jenks et al., 1994; M.A. Jenks, unpublished data). By comparison, it seems unlikely that alteration in the cuticle membrane ultrastructure of *wax2* could have caused such a large reduction in wax amount on *wax2*. Cuticle membrane alteration also would not be expected to suppress just one branch of the wax synthetic pathway, as occurs on *wax2* (i.e., *wax2* primarily inhibits the conversion of acyl-CoAs to aldehydes, as discussed below). Also, *wax2*'s outer epidermal cell walls were much more darkly stained with osmium (as reported for sorghum *bm2*), suggesting the accumulation of new materials. Whether these new cell wall deposits represent the accumulation of cuticle precursors or secreted proteins required for cuticle synthesis is uncertain. Potentially, WAX2 plays a role in the conversion or secretion of cuticle lipid precursors common to both cutin and wax pathways.

The predicted WAX2 protein has 32 and 35% sequence identity to the predicted Arabidopsis CER1 and maize GL1 proteins, respectively, and mutations in both *CER1* and *GL1* cause dramatic alterations in the amount, composition, and crystallization patterns of their cuticular waxes (Lorenzoni and Salamini, 1975; Bianchi et al., 1985; Jenks et al., 1995). Aarts et al. (1995) predicted that *CER1* could code for a putative plant decarbonylase, because *cer1* is proportionally deficient only in alkanes (and alkane-derived metabolites) and had increased aldehydes, and that the CER1 protein had metal binding motifs found in other lipid-synthesizing proteins (Cheesbrough and Kolattukudy, 1984; Dennis and Kolattukudy, 1992). In contrast to *cer1*, the stems of *wax2* are deficient in both aldehydes and alkanes (and its metabolites), suggesting that *wax2*'s primary blockage (Figure 10) occurs in the metabolic step preceding that blocked by *cer1*. Conversely, Hansen et al. (1997) suggested that the homologous *GL1* could not code for a decarbonylase because

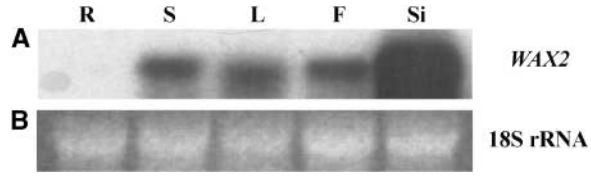

Figure 6. Expression of *WAX2* in Wild-Type Arabidopsis Ecotype C24.

(A) RNA gel blot analysis of total RNA prepared from roots (R), stems (S), leaves (L), flowers (F), and siliques (Si) of wild-type C24 plants.
(B) 18S rRNA bands on an ethidium bromide–stained gel of the corresponding lanes in **(A)**.

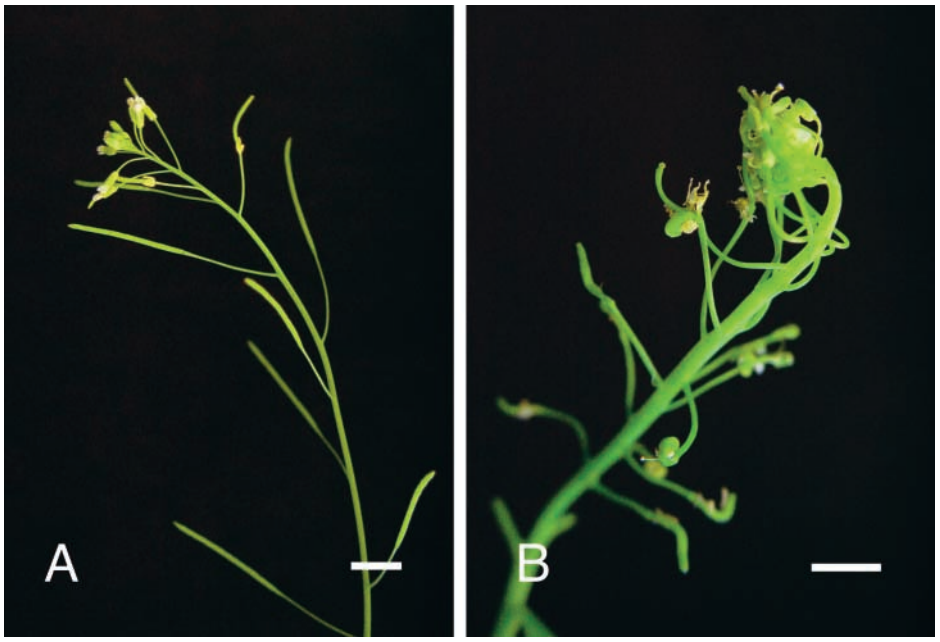

Figure 7. Terminal Inflorescences of Arabidopsis Ecotype C24 and the *wax2* Mutant.

(A) Arabidopsis wild-type C24 siliques showing normal elongated morphology, representing full fertility. Postgential fusion does not occur in ecotype C24. Bar = 6 mm.

(B) Arabidopsis *wax2* mutant showing stunted siliques, representing near or total seedlessness. Typical postgenital fusions often occur between the abaxial sepal surfaces of flower buds. Fusion occurs between many other aerial organs as well (data not shown). Bar = 6 mm.

the *gl1* mutant actually had higher proportions of alkanes than the wild-type parent and the GL1 protein lacked the third His-rich motif required for iron binding. Instead, based on the predicted secondary structure of GL1 and CER1, Hansen et al. (1997) suggested that these proteins might belong to a superfamily of integral membrane receptors that are composed of a hydrophobic N-terminal domain with seven transmembrane-spanning regions and a globular water-soluble C-terminal domain (Probst et al., 1992). Although WAX2, CER1, and GL1 have comparable transmembrane structures, our analysis using Sequence BLAST and multiple alignments using CLUSTAL W 1.82 did not show high similarity to membrane receptors.

Our analysis (like that of Aarts et al., 1995) indicates that WAX2 is homologous with lipid metabolic proteins. The WAX2 amino acid sequence was 95.4% aligned with the signature sequence (CD length of 216 residues) of the sterol desaturase family at the N-terminal end and contained the three His-rich motifs conserved in this family. These His-rich motifs are associated with diiron-oxo binding and are required for catalytic activity in enzymes such as fatty acyl desaturase, alkane ω-hydroxylase, xylene monooxygenase, C-5 desaturase, and C-4 sterol methyl oxidase (Fox et al., 1994; Shanklin et al., 1994, 1997; Bard et al., 1996; Gachotte et al., 1996). The C-terminal end of WAX2 (residues 456 to 497) was 16.7% aligned with the signature sequence (CD length of 252 residues) of the SDR. The homology with SDR existed only in WAX2 (and Rice and *Senecio* WAX2 homologs) and not in GL1, CER1, and CER1-like proteins. The SDR family contains a wide variety of dehydrogenases, most of which are known to be NAD- or NADP-dependent oxidoreductases. Members of this SDR family include acetoacetyl-CoA dehydrogenase, 3-oxoacyl(acyl-carrier protein) reductase, NADH-dependent carbonyl reductase, alcohol dehydrogenase, D-β-hydroxybutyrate dehydrogenase, and retinol dehydrogenase (from PROSITE, http://ca.expasy.org/cgi-bin/prosite-search-ac?PDOC00060).

Potentially, *wax2*'s effect on both cuticle membrane and wax pathways might be explained if WAX2 is a fusion of two functional proteins containing both sterol desaturase and SDR domains that play separate roles in each part. These separate domains in *WAX2* even appear to include the conserved residues essential for distinct catalytic function. Previously, a single gene from yeast was shown to encode a cytochrome b_5 sequence fused to the C-terminal domain of a Δ^9-18:0-CoA desaturase (Mitchell and Martin, 1995), and single genes from both yeast and plants have cytochrome b_5 at the N terminus of a sphingolipid desaturase (Mitchell and Martin, 1997; Sperling et al., 1998). An alternative hypothesis is that WAX2 possesses a single catalytic site capable of more than one kind of reaction. Xylene monooxygenase (of the sterol desaturase family) from *Escherichia coli* catalyzes each step in the oxygenation of toluene and pseudocumene to the corresponding alcohols, aldehydes, and acids (Buhler et al., 2000), and oleate hydroxylase from *Lesquerella fendleri* has both hydroxylase and desaturase activities (Broun et al., 1998a, 1998b). Broun et al. (1998b) showed how only seven residues were strictly conserved in a comparison among six desaturases. Interestingly, as few as four amino acid substitutions converted a strict desaturase to

Table 2. Arabidopsis Ecotype C24 and Mutant *wax2* Stomatal and Pavement Cell Densities and Stomatal Index of Adult-Phase Leaf Blades

Surface	Stomatal Density (cells/mm^2 ± SD)	Pavement Cell Density (cells/mm^2 ± SD)	Stomatal Index	Percent Change in Stomatal Index
Adaxial				
C24	101 ± 11.3	243 ± 18.4	29.4 ± 1.0	
wax2	87 ± 19.0	265 ± 79.3	24.7 ± 2.2	−16.0
Abaxial				
C24	148 ± 22.5	358 ± 84.4	29.3 ± 2.3	
wax2	105 ± 12.8	329 ± 36.6	24.2 ± 1.5	−17.4

an enzyme that retained some desaturase activity but also was an efficient hydroxylase, and as few as six amino acid substitutions increased desaturation activity in a hydroxylase.

The broad range of activities and catalytic plasticity associated with both the sterol desaturase and SDR families, and the cuticle properties of the *wax2* mutant, lead us to speculate that WAX2 may participate in the modification of more than one cuticle lipid substrate. Specifically, WAX2 could be a multifunctional enzyme involved in both the reduction of acyl-CoAs to aldehydes (which is required for the synthesis of alkane and its metabolites) and the hydroxylation of acyl-CoAs to certain cutin monomers (Figure 10). However, additional studies are needed.

WAX2 Contributes to the Suppression of Postgenital Fusion

The *wax2* mutant often displays postgenital fusion. Likewise, the glossy-stemmed Arabidopsis mutants *wax1* (Jenks et al., 1996) and *ded* (Lolle et al., 1998) and the semiglaucous mutants *cer10* and *cer13* have organs that undergo postgenital fusion. Fusion in *wax2*, *cer10*, and *cer13* is less severe than that in *wax1* and *ded*. Other Arabidopsis mutants that show postgenital fusion are *ahd*, *bud*, *cod*, *fdh*, *hth*, *phd*, *thd* (Lolle et al., 1998), and *lcr* (Wellesen et al., 2001). However, none of these mutants has altered visible wax deposition. Interestingly, the *FDH* and *LCR* genes were cloned and found to encode putative cuticle lipid-synthesizing enzymes (Yephremov et al., 1999; Pruitt et al., 2000; Wellesen et al., 2001). Whether these fusion mutants with normal glaucousness have changes in their cuticle ultrastructures or compositions has not been reported. Ectopic expression of the cutinase gene from *Fusarium solani* f.sp. *pisi* in Arabidopsis led to altered cuticle membrane ultrastructure, increased cutin monomers, and postgenital fusion (Sieber et al., 2000), providing additional evidence for cutin involvement in fusion. In *wax2*, fully expanded leaves do not fuse upon physical contact, suggesting that fusion competence occurs in primordial or young organs. Potentially, postgenital fusion by *wax2* could be caused by a delay or reduction in cuticle deposition early in organ formation. In the wild type, the cuticle itself could act as the suppressor of postgenital fusion by blocking the diffusion of morphogenic signal compounds that normally function in cell-to-cell fusion, as occurs between carpels (Verbeke and Walker, 1986). Alternatively, WAX2 itself could synthesize lipids involved in signaling epidermal development. Further studies of cuticle involvement in the regulation of plant development are needed.

WAX2 Plays a Conditional Role in Pollen Fertility

Like certain cuticular wax mutants in Arabidopsis (Koornneef et al., 1989), *wax2* shows severe male sterility in low-humidity environments that can be overcome in high humidity. Similarly, reduced fertility in *cer1* and *cer6* also was male gamete specific and associated with the alteration of certain pollen coat lipids (Preuss et al., 1993; Aarts et al., 1995; Fiebig et al., 2000). Evidence that altered pollen lipids disrupt normal pollen-stigma communication includes the following: (1) *cer1* and *cer6* pollen induces noncompatibility reactions (callose synthesis) in normally compatible stigmas; (2) wild-type, *cer1*, and *cer6* pollen germinate in an artificial medium equally well; and (3) wild-type, *cer1*, and *cer6* pollen placed on the same stigma induce the secretion of stigma water, leading to pollen hydration and almost normal development of the wild-type and mutant pollen. It has been proposed that altered pollen lipid composition and ultrastructure may disrupt pollen-stigma communication, but a detailed study of most pollen lipid components (such as cutin,

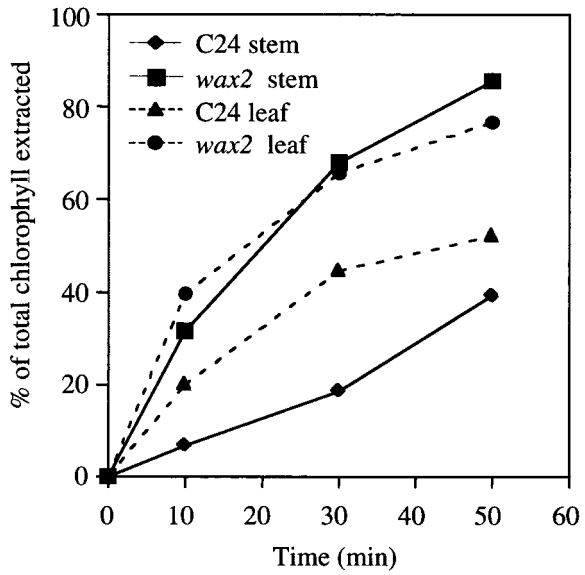

Figure 8. Permeability to Chlorophyll by Arabidopsis Ecotype C24 and the *wax2* Mutant.

Stems and leaves of *wax2* show higher permeability to chlorophyll than those of the wild type. Total chlorophyll is represented as a percentage of the total extractable chlorophyll (as described by Lolle et al., 1998).

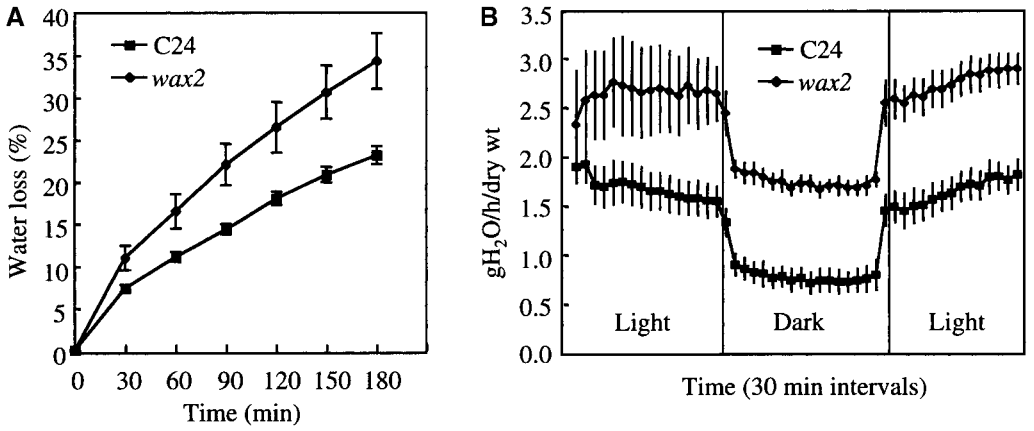

Figure 9. Transpiration Rates (±SD) of Arabidopsis Ecotype C24 and the *wax2* Mutant.

(A) Excised stem water loss rates recorded over 180 min measured as a percentage of the initial weight of fully hydrated stems.
(B) Whole flowering plant in-pot transpiration rates in both light and dark. Response time to the light and dark treatments is identical in both lines, indicating that *wax2* stomata have a normal response to light.

wax esters, shorter chain lipids, and others) has not been reported. Also, whether the deficiency in lipid globules of the *cer6* exine (which is visible by transmission electron microscopy) is attributable to a reduction in waxes is doubtful, because long-chain waxes typically form crystalline structures. Recent reports that *cis*-unsaturated triacylglycerides may serve as stigma-pollen recognition signals (Wolters-Arts et al., 1998) raise intriguing questions about the role of these wax gene products in synthesizing fertility-regulating signaling compounds. Whether *wax2* alters the synthesis of signaling compounds, or simply changes pollen or stigma permeability to the diffusion of other signaling molecules, is an important question for future studies.

WAX2 Affects Epidermal Permeability

The Arabidopsis *wax2* mutant had increased transpiration rates relative to the wild type, both when stomata were assumed primarily open (in light) and when stomata were assumed closed (in dark), even though *wax2* has fewer stomata. The response time for light-induced changes in transpiration were identical in the wild type and *wax2*, indicating that stomatal function in this respect is normal. Relative to the wild type, chlorophyll is extracted more rapidly from leaves and stems of *wax2*, and the *wax2* mutant shows higher susceptibility to two foliarly applied herbicides, indicating that larger molecules than water also penetrate the cuticle more easily. Increased epidermal permeability to both water and larger compounds by *wax2* was not unexpected, because Niederl et al. (1998) suggested that water and organic compounds such as the herbicide 2,4-D diffuse along identical amorphous pathways in the cuticle. Exactly how diffusion pathways have changed in *wax2* remains unclear. *wax2* has reduced visible density in the cuticle membrane, suggesting that the internal molecular packing of cuticle lipid molecules may be less dense. If this is so, the proportion of crystalline regions in the cuticle, which serve as exclusion zones for diffusion (Baur et al., 1999), may be reduced, leading to more direct pathways for water diffusion through *wax2* cuticles. The effect of *wax2* on cuticles that overlie the stomatal ridges, pores, or substomatal chambers (Osborn and Taylor, 1990; Zhao and Sack, 1999) or the inner epidermis adjacent to the mesophyll (Pesacreta and Hasenstein, 1999) is unknown. Studies to assess the relative impact of *wax2* on the permeability of cuticle membranes associated with epidermal pavement cells (inner and outer surfaces) and the stomatal complexes are needed to provide a more complete understanding of *wax2*'s effects on plant water relations and epidermal permeability.

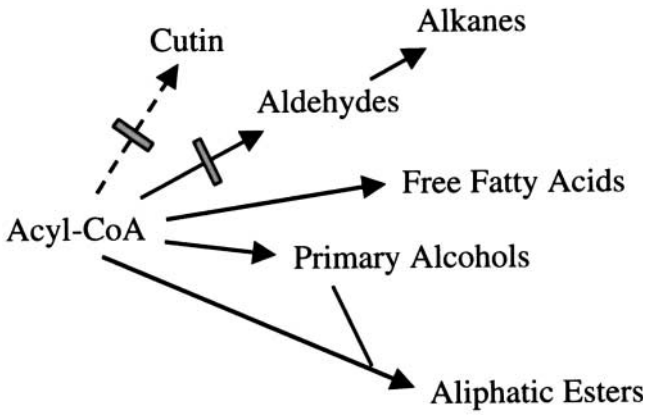

Figure 10. Model Pathway for Acyl-CoA Conversion in Cuticle Lipid Metabolism.

Long-chain acyl-CoAs serve as substrates in the synthesis of cuticle lipids (Kolattukudy, 1996). The *wax2* mutation primarily blocks the synthesis of aldehydes and their metabolites, suggesting that WAX2 may function in acyl-CoA reduction. *wax2*'s cuticle membrane disruption and the WAX2 protein's homology with hydroxylases suggest that WAX2 also may be required for cutin synthesis.

WAX2 Affects Epidermal Architecture

Wax mutants often possess altered stomata. For example, leaf surfaces of Arabidopsis *cer1* and *cer6* mutants have higher stomatal indices than those of their isogenic wild-type parent (Gray et al., 2000), and 12 mutant alleles of the *cer-g* locus in barley have abnormal stomatal morphology (Zeiger and Stebbins, 1972). By contrast, *wax2* has a lower stomatal index than the wild type. As opposed to stomatal density, which could be changed by differences in leaf and cell expansion, the stomatal index describes the number of stomata as a function of total cell number. Thus, fewer stomata (and more pavement cells) were initiated in the leaf primordium of *wax2* than in the wild type. Whether *wax2* cuticle alterations influence the synthesis or diffusion of chemical signals that direct stomatal initiation during epidermal development is the subject of ongoing studies. Interestingly, WAX2 plays a role in the formation of both the cuticle and the stomata, two epidermal traits critically involved in transpirational control and, ultimately, plant drought tolerance.

Conclusions

The *wax2* mutation identified a novel gene that functions in both cuticle membrane and cuticle wax production. Our studies reveal a possible role for the cuticle as a suppressor of organ fusion early in organ formation and provide further evidence for a connection between the cuticle and both fertility and the development of epidermal architecture (via effects on the stomatal index). Whether these functions are associated with genetics, chemical signaling, physical effects, or other mechanisms remains unclear. The *WAX2* gene is homologous with Arabidopsis *CER1*. However, mutation in *CER1* alters wax but not the cuticle membrane. Comparisons of the predicted *WAX2*, *CER1*, and *GL1* proteins, and the phenotypes of their respective mutants, lead us to predict that the *WAX2* gene product has a metabolic function. Further studies of *WAX2* are needed to provide a better understanding of gene involvement in plant cuticle production and to advance our understanding of the cuticle's role in plant development.

METHODS

Genetic Analysis of *wax2*

The activation T-DNA vector pSKI015 was used to generate an insertion mutant population (T1) in the genetic background of *Arabidopsis thaliana* ecotype C24 as described by Weigel et al. (2000). Bialophos resistance was used as the selectable marker. Plants were grouped into pools of 10 families, and T2 progeny of ~200 plants from these pools were screened for mutants with reduced visible glaucousness of the inflorescence stem surface. Mutagenized populations were grown in a greenhouse at Purdue University using overhead irrigation, natural light, and a temperature of ~22°C. The original mutants were given a secondary screen for water loss from excised stems and whole plant transpiration rates (see below). Mutants with high transpiration rates were examined subsequently for changes in cuticle membrane weight and ultrastructure (see below).

Analysis of the Cuticle Membrane

The cuticle and outer cell wall ultrastructures of inflorescence stems and abaxial and adaxial leaf epidermises of 6-week-old plants were viewed by transmission electron microscopy. Stem specimens were collected from the middle of the first (lowest) internode, whereas leaf samples were collected from the middle of the blade between the midvein and the margin of leaf 8. The samples were fixed for 1 h at room temperature in primary fixative containing 2.5% (v/v) glutaraldehyde and 2% (v/v) formaldehyde in 0.05 M phosphate buffer, pH 6.8 (PB) (Karnovsky, 1965). A microwave oven (model 3450; Ted Pella, Redding, CA) with vacuum was used to improve cuticle fixation. Various microwave treatments were tested and compared with standard fixation at room temperature; two 40-s microwave treatments using the low power setting, with a 3-min period between the two exposures, provided excellent preservation. After fixation, samples were washed with PB and postfixed for 1 h in 2% (v/v) osmium tetroxide in 0.05 M PB. One 40-s microwave treatment with vacuum as described above was applied during osmium fixation. After washing with PB, the tissues were dehydrated through a gradient series of ethanol, infiltrated with Spurr's embedding medium (Electron Microscopy Sciences, Fort Washington, PA), and polymerized for 48 h at 60°C. Ultrathin sections (80 to 100 nm) were prepared from Spurr's resin–embedded samples and mounted on carbon-coated Formvar 100-mesh copper grids (Electron Microscopy Sciences). Sections were air-dried, stained at room temperature with 2% (v/v) uranyl acetate for 5 min, and then stained with lead citrate for 3 min before viewing with a Philips EM 400 electron microscope (FEI Co., Hillsboro, OR).

Gravimetric measurements of cuticle membrane weight were determined for wild-type and *wax2* inflorescence stem samples collected from the first internodes of 6-week-old plants. After removing soluble cuticular waxes by means of a 30-s dip in hexane, stem samples were soaked for 8 h in a 60% (w/v) solution of ZnCl in HCl to separate cuticle membranes from underlying stem tissues (Jenks et al., 1994). Bulk samples of 30 stem cuticle membranes (separated with a dissecting microscope) were placed on glass microscope cover slips, oven-dried at 50°C, and then placed in a desiccator containing dried silica gel for at least 12 h. Average cuticle membrane weights per surface area (stem segment circumference times height) for each line were determined from six replicate bulk samples using a microbalance. Leaf cuticles regularly broke up during ZnCl-HCl treatments, especially those of *wax2*. For that reason, leaf cuticle weights were not determined.

Analysis of Cuticular Waxes

Scanning electron microscopy was used to analyze epicuticular wax crystallization patterns. Leaf and stem (first internode above the rosette) samples were collected from Arabidopsis wild-type and *wax2* plants after 6 weeks of growth. Four replicates of each sample were mounted on aluminum stubs and sputter-coated with gold palladium using six 30-s bursts from the sputter coater. Previous research showed that air-dried samples coated in this way were similar to specimens prepared using low-temperature scanning electron microscopy with little evidence of artifacts in wax crystallization patterns (Jenks et al., 1992). Coated surfaces were viewed using a JEOL JSM-840 scanning electron microscope at 5 kV.

For compositional analysis, cuticular wax samples were extracted from the leaves and stems of flowering Arabidopsis wild-type and *wax2* plants after 6 weeks of growth. Leaf and stem (representing the first through fifth internodes) samples were inserted into a 20-mL standard glass scintillation vial, and ~15 mL of gas chromatography–grade hexane was added. The tissues were agitated for 30 s, and the solvent was decanted into new scintillation vials. Tissues and vials were given a 1-s rinse with approximately 2 mL of hexane, and then the solution was de-

canted into the sample vial. Thus, the leaf extracts contain waxes from both abaxial and adaxial leaf surfaces and, like stems, showed little or no coloration as a result of chlorophyll or other internal lipids. Wax compositional analysis was performed according to Jenks et al. (1995). The hexane-soluble cuticular wax extracts were evaporated to dryness under a nitrogen stream, and the dried residue was prepared for gas chromatography by derivatization using *N*,*O*-bis(trimethylsilyl)trifluoroacetamide. Derivatization was for 15 min at 100°C. After surplus *N*,*O*-bis(trimethylsilyl)trifluoroacetamide was evaporated under nitrogen, the sample was redissolved in hexane for analysis with a Hewlett-Packard 5890 series II gas chromatograph equipped with a flame ionization detector (Palo Alto, CA). The gas chromatograph was equipped with a 12-m, 0.2-mm HP-1 capillary column with helium as the carrier gas. The gas chromatograph was programmed with an initial temperature of 80°C and increased at 15°C/min to 260°C, at which point the temperature remained unchanged for 10 min. The temperature then was increased at 5°C/min to 320°C, at which point the temperature was held for 15 min.

Quantification was based on flame ionization detector peak areas and the internal standard hexadecane. Specific correction factors were developed from external standards and applied in a standard manner as described by Jenks et al. (1995, 1996). The total amount of cuticular wax was expressed per unit of stem or leaf surface area. Stem surface areas were calculated as the surface area of a right circular cylinder, and leaf areas were determined using computer digitization (NIH Image version 1.62). All values represent averages of four replicate plant samples ± SD. Selected subsamples were used for injection in a gas chromatograph–mass spectrometer (FinniganMAT/Thermospray Corp., San Jose, CA) to produce electron ionization mass spectra to verify the identities of all components.

Plasmid Rescue and Linkage Analysis

Plasmid rescue was performed according to Weigel et al. (2000). The restriction enzymes EcoRI and HindIII were used to rescue the right T-DNA border flanking sequences, and BamHI was used for left border rescue. The rescued sequences were sequenced directly from both ends using primers designed from inside the restriction site sequences and the T-DNA border sequences. The flanking gene-specific DNA sequence was searched against the Arabidopsis genome database (http://www.ncbi.nlm.nih.gov/PMGifs/Genomes/ara.html). A primer pair designed from the rescued T-DNA and flanking gene-specific sequence (SKIAV, 5′-TCACGGATCGACTGCTTCT-3′; and P2, 5′-CACTTCTGCTACACTCTACT-3′) and a primer pair across the insertion designed from At5g57800 (P1, 5′-TTCTTCACACATTACCACTCT-3′; and P2) were used for PCR analysis of the *wax2-1* backcross F2 population for linkage between the tagged sequence and the mutant phenotype. The PCR primers used to check the linkage between *wax2-2*'s visible mutant phenotypes and the flanking T-DNA were P3 (5′-AGATTGATCACGAATGGCACT-3′) and P4 (5′-TTTCCAATAACGTTGCGTTTC-3′) from the *WAX2* gene and GarlicLB2 (5′-ATCTTCCCAAATTACCAATACA-3′) from the T-DNA left border.

5′ and 3′ Rapid Amplification of cDNA Ends

The full-length cDNA clone was obtained by 5′ and 3′ rapid amplification of cDNA ends (RACE) using the SMART RACE cDNA Amplification Kit (BD Biosciences Clontech, Palo Alto, CA) as described by the manufacturer. The gene-specific primers used for RACE were designed from the EST and the At5g57800 putative mRNA sequence. The primers for 5′ RACE were 5R1 (5′-TCCTGCTTGCATCTCCTTTCACCTG-3′) and 5R2 (5′-GGCTCCAGTCAAGAAAACCTC-3′). The primers for 3′ RACE were P1 and 3R2 (5′-GTGCCGGAGTTTGTGTTCTTA-3′). The PCR fragments were cloned into the pGEM-T Easy vector (Promega, Madison, WI).

DNA and RNA Gel Blot Analysis

Genomic DNA was isolated from rosette leaves according to Dellaporta et al. (1983) with minor modifications. DNA was digested using three restriction enzymes, HindIII, BamHI, and EcoRI, and fractionated using electrophoresis. A *BAR* gene fragment was used as a DNA probe. The probe was labeled with α-^{32}P-dCTP (DuPont–New England Nuclear) using the random prime labeling kit (Decaprime II; Ambion, Austin, TX). Membranes were washed at 42°C in 2× SSC (1× SSC is 0.15 M NaCl and 0.015 M sodium citrate) and 0.1% SDS twice for 5 min followed by washing in 0.1× SSC and 0.1% SDS twice for 15 min.

Total RNA was isolated from various tissues using the RNeasy Plant Mini Kit (Qiagen, Valencia, CA) as described by the manufacturer. RNA gel blot analysis was performed according to standard methods. The 1.8-kb EcoRI-digested fragment from the 5′ RACE product was used as a probe, with probe labeling and hybridization the same as for the DNA blot.

Bioinformatics

Multiple sequence alignment was performed with CLUSTAL W (Thompson et al., 1994) using default parameters through BCM Search Launcher (http://searchlauncher.bcm.tmc.edu/multi-align/multi-align.html). The boxshade was created by BOXSHADE 3.21 (http://www.ch.embnet.org/software/BOX_form.html). The rooted phylogenetic tree was constructed using CLUSTAL W (Thompson et al., 1994). Transmembrane analysis was performed using TMHMM (http://www.cbs.dtu.dk/services/TMHMM/).

Quantifying Epidermal Traits of the Wild Type and *wax2*

To quantify excised stem water loss rates, stems of 6-week-old plants were excised and the cauline leaves were removed. The stems were placed immediately in water (in the dark) and soaked for 60 min. Stems removed from soaking were shaken gently and blotted to remove excess water, suspended in complete darkness, and weights were determined gravimetrically every 30 min using a microbalance. For whole plant transpiration measurements, flowering plants were grown in 3-inch pots enclosed in polyethylene bags and bound either over or under the rosette to prevent water loss except through the exposed plant surfaces. The contact point between the bag and the stem or crown was sealed with Parafilm to prevent water loss between the plant and the pot enclosure. Allowing 8 h for plant transpiration rates to stabilize, transpiration rates of three wild-type and three *wax2* replicates were monitored instantaneously using six electronic balances and WinWedge data-acquisition software (TalTech, Philadephia, PA). To increase water loss amounts to improve measurement accuracy, three plants placed on one balance constituted one replicate. Measurements were performed in complete darkness (when stomata were assumed generally closed) and in the light (when stomata were assumed generally open). A 400-W metal halide lamp provided illumination (120 μmol·m^{-2}·s^{-1}). Temperature during the study ranged from 27 to 28°C, and RH was between 32 and 42%. Short-term responsiveness of transpiration to light-dark transitions was monitored as a means of describing stomatal responsiveness. Excised stem water loss also was examined in segregating populations, as described by Jenks et al. (1994), between the wild type and *wax2* to verify that high water loss cosegregated with the visible phenotypes (see above).

Epidermal permeability also was measured using chlorophyll efflux and foliarly applied herbicide sensitivity studies. Twenty whole preflowering rosettes and stem first internodal segments were collected from 4- and 6-week-old plants, respectively, and immersed in an 80% ethanol solution in glass scintillation vials. Vials were covered with aluminum foil

and agitated gently on a shaker platform. Aliquots of 100 μL were removed at 10 min, 30 min, 50 min, and 24 h after initial immersion. The amount of chlorophyll extracted into the solution was quantified using a UV-2102 PC spectrophotometer (UNICO, Dayton, NJ) and calculated from UV light absorption at 647 and 664 nm as described by Lolle et al. (1998). Total chlorophyl was expressed for each time point as a percentage of total chlorophyll extracted after 24 h. Herbicide sensitivity of the wild type and *wax2* was determined for two herbicides, paraquat and acifluorfen, after initial dose-response curves were established for the wild type to approximate 50% lethal dose levels. Seven replicates of each line were treated with doses just above the 50% lethal dose. Injury was scored visually by three investigators over a 48-h time course according to a modified Horsfall-Barret scale (0 to 10, with 0 indicating no damage and 10 representing 100% of tissue showing any discoloration).

Stomatal density, epidermal pavement cell density, and stomatal index for both the adaxial and abaxial surfaces were determined using light microscopy modified according to Gray et al. (2000). Instead of dental rubber impressions, we created imprints using Duro Super Glue (Loctite, Avon, OH; cyanoacrylate) of 1.01-mm^2 areas taken from the middle of the leaf blade between the midrib and the margin. Leaves were selected for uniform size, being numbered 20 to 23 from the first true leaves, and the plants were 39 days old. Values for stomatal index presented for each surface represent the average of at least 9 to 12 replicate imprints.

Upon request, all novel materials described in this article will be made available in a timely manner for noncommercial research purposes.

Accession Numbers

The GenBank accession number for the *WAX2* nucleotide sequence is AY131334. Other accession numbers are as follows: At5g57800, NM125164; *epi23*, L33792; partial rice sequence annotated as a GLOSSY1 homolog, T04146; maize GLOSSY1, U37428; Arabidopsis CER1, U40489; *Senecio odorus* partial protein sequence, L33792; Arabidopsis CER1L19, X95965; and *Schizosaccharomyces pombe* C-4 methyl sterol oxidase of the desaturase family, T38986.

ACKNOWLEDGMENTS

We thank Syngenta for providing the T-DNA mutant line SAIL 832 E06 and the Salk Institute Genomic Analysis Laboratory for providing the sequence-indexed Arabidopsis T-DNA insertion mutant (SALK 034318). We also thank Debra Sherman of the Purdue University Electron Microscopy Center. This article is publication 16904 of the Purdue University Office of Agricultural Research.

Received January 31, 2003; accepted March 7, 2003.

REFERENCES

Aarts, M.G., Keijzer, C.J., Stiekema, W.J., and Pereira, A. (1995). Molecular characterization of the *CER1* gene of Arabidopsis involved in epicuticular wax biosynthesis and pollen fertility. Plant Cell **7,** 2115–2127.

Bard, M., Bruner, D.A., Pierson, C.A., Lees, N.D., Biiermann, B., Frye, L., Koegel, C., and Barbuch, R. (1996). Cloning and characterization of ERG25, the *Saccharomyces cerevisiae* gene encoding C-4 sterol methyl oxidase. Proc. Natl. Acad. Sci. USA **93,** 186–190.

Baur, P., Marzouk, H., and Schönherr, J. (1999). Estimation of path lengths for diffusion of organic compounds through leaf surfaces. Plant Cell Environ. **22,** 291–299.

Becraft, P.W., Kang, S.H., and Suh, S.G. (2001). The maize *CRINKLY4* receptor kinase controls a cell-autonomous differentiation response. Plant Physiol. **127,** 486–496.

Benveniste, I., Tijet, N., Adas, F., Philipps, G., Salaun, J.P., and Durst, F. (1998). *CYP86A1* from *Arabidopsis thaliana* encodes a cytochrome P450-dependent fatty acid omega-hydroxylase. Biochem. Biophys. Res. Commun. **243,** 688–693.

Bianchi, A., Bianchi, G., Avato, P., and Salamini, F. (1985). Biosynthesis pathways of epicuticular wax of maize as assessed by mutation, light, plant age and inhibitor studies. Maydica **30,** 179–198.

Broun, P., Boddupalli, S., and Somerville, C. (1998a). A bifunctional oleate 12-hydroxylase:desaturase from *Lesquerella fendleri*. Plant J. **13,** 201–210.

Broun, P., Shanklin, J., Whittle, E., and Somerville, C. (1998b). Catalytic plasticity of fatty acid modification enzymes underlying chemical diversity of plant lipids. Science **282,** 1315–1317.

Buhler, B., Schmid, A., Hauer, B., and Witholt, B. (2000). Xylene monooxygenase catalyzes the multistep oxygenation of toluene and pseudocumene to corresponding alcohols, aldehydes, and acids in *Escherichia coli* JM101. J. Biol. Chem. **275,** 10085–10092.

Cheesbrough, T.M., and Kolattukudy, P.E. (1984). Alkane biosynthesis by decarbonylation of aldehydes catalyzed by a particulate preparation from *Pisum sativum*. Proc. Natl. Acad. Sci. USA **81,** 6613–6617.

Dennis, M., and Kolattukudy, P.E. (1992). A cobalt-porphyrin enzyme converts a fatty aldehyde to a hydrocarbon and CO. Proc. Natl. Acad. Sci. USA **89,** 5306–5310.

Dellaporta, S.L., Wood, V.P., and Hicks, J.B. (1983). A plant DNA minipreparation: Version II. Plant Mol. Biol. Rep. **1,** 19–21.

Eigenbrode, S.D., and Espelie, K.E. (1995). Effects of plant epicuticular lipids on insect herbivores. Annu. Rev. Entomol. **40,** 171–194.

Fiebig, A., Mayfield, J.A., Miley, N.L., Chau, S., Fischer, R.L., and Preuss, D. (2000). Alterations in *CER6*, a gene identical to *CUT1*, differentially affect long-chain lipid content on the surface of pollen and stems. Plant Cell **12,** 2001–2008.

Fox, B.G., Shanklin, J., Ai, J., Loehr, T.M., and Sanders-Loehr, J. (1994). Resonance Raman evidence for an Fe-O-Fe center in stearoyl-ACP desaturase: Primary sequence identity with other diiron-oxo proteins. Biochemistry **33,** 12776–12786.

Gachotte, D., Husselstein, T., Bard, M., Lacroute, F., and Benveniste, P. (1996). Isolation and characterization of an *Arabidopsis thaliana* cDNA encoding a delta 7-sterol-C-5-desaturase by functional complementation of a defective yeast mutant. Plant J. **9,** 391–398.

Gray, J.E., Holroyd, G.H., van der Lee, F.M., Bahrami, A.R., Sijmons, P.C., Woodward, F.I., Schuch, W., and Hetherington, A.M. (2000). The *HIC* signaling pathway links CO_2 perception to stomatal development. Nature **408,** 713–716.

Hannoufa, A., Negruk, V., Eisner, G., and Lemieux, B. (1996). The *CER3* gene of *Arabidopsis thaliana* is expressed in leaves, stems, roots, flowers and apical meristems. Plant J. **10,** 459–467.

Hansen, J.D., Pyee, J., Xia, Y., Wen, T.J., Robertson, D.S., Kolattukudy, P.E., Nikolau, B.J., and Schnable, P.S. (1997). The *GLOSSY1* locus of maize and an epidermis-specific cDNA from *Kleinia odora* define a class of receptor-like proteins required for the normal accumulation of cuticular waxes. Plant Physiol. **113,** 1091–1100.

Jeffree, C.E. (1996). Structure and ontogeny of plant cuticles. In Plant Cuticles: An Integrated Functional Approach, G. Kerstiens, ed (Oxford, UK: BIOS Scientific Publishers), pp. 33–82.

Jenks, M.A. (2002). Critical issues with the plant cuticle's function in drought tolerance. In Biochemical & Molecular Responses of Plants to the Environment, A.J. Wood, ed (Kerala, India: Research Signpost Press), pp. 97–127.

Jenks, M.A., and Ashworth, E.N. (1999). Plant epicuticular waxes: Function, production, and genetics. Hortic. Rev. **23,** 1–68.

Jenks, M.A., Eigenbrode, S., and Lemeiux, B. (2002). Cuticular waxes of Arabidopsis. In The Arabidopsis Book, C. Somerville and E. Meyerowitz, eds (Rockville, MD: American Society of Plant Biologists), doi/10.1199/tab.0016, http://www.aspb.org/publications/arabidopsis.

Jenks, M.A., Joly, R.J., Peters, P.J., Rich, P.J., Axtell, J.D., and Ashworth, E.A. (1994). Chemically-induced cuticle mutation affecting epidermal conductance to water vapor and disease susceptibility in *Sorghum bicolor* (L.) Moench. Plant Physiol. **105,** 1239–1245.

Jenks, M.A., Rashotte, A.M., Tuttle, H.A., and Feldmann, K.A. (1996). Mutants in *Arabidopsis thaliana* altered in epicuticular wax and leaf morphology. Plant Physiol. **110,** 377–385.

Jenks, M.A., Rich, P.J., Peters, P.J., Axtell, J.D., and Ashworth, E.N. (1992). Epicuticular wax morphology of *bloomless* (*bm*) mutants in *Sorghum bicolor*. Int. J. Plant Sci. **153,** 311–319.

Jenks, M.A., Rich, P.J., Rhodes, D., Ashworth, E.A., Axtell, J.D., and Ding, C.K. (2000). Chemical composition of leaf sheath cuticular waxes on *bloomless* and *sparse-bloom* mutants of *Sorghum bicolor* (L.) Moench. Phytochemistry **54,** 577–584.

Jenks, M.A., Tuttle, H.A., Eigenbrode, S.D., and Feldmann, K.A. (1995). Leaf epicuticular waxes of the *eceriferum* mutants in *Arabidopsis*. Plant Physiol. **108,** 369–377.

Jin, P., Guo, T., and Becraft, P.W. (2000). The maize *CR4* receptor-kinase mediates a growth factor-like differentiation response. Genesis **27,** 104–116.

Karnovsky, M.J. (1965). A formaldehyde-glutaraldehyde fixative of high osmolarity for use in electron microscopy. J. Cell Biol. **27,** 137A.

Kolattukudy, P.E. (1996). Biosynthetic pathways of cutin and waxes: their sensitivity to environmental stresses. In Plant Cuticles: An Integrated Functional Approach, G. Kerstiens, ed (Oxford, UK: BIOS Scientific Publishers), pp. 83–108.

Koornneef, M., Hanhart, C.J., and Thiel, F. (1989). A genetic and phenotypic description of *eceriferum* (*cer*) mutants in *Arabidopsis thaliana*. J. Hered. **80,** 118–122.

LeBouquin, R., Pinot, F., Benveniste, I., Salaun, J.P., and Durst, F. (1999). Cloning and functional characterization of *CYP94A2*, a medium chain fatty acid hydroxylase from *Vicia sativa*. Biochem. Biophys. Res. Commun. **261,** 156–162.

Lolle, S.J., Hsu, W., and Pruitt, R.E. (1998). Genetic analysis of organ fusion in *Arabidopsis thaliana*. Genetics **149,** 607–619.

Lorenzoni, C., and Salamini, F. (1975). Glossy mutants of maize. V. Morphology of the epicuticular waxes. Maydica **20,** 5–19.

Millar, A.A., Clemens, S., Zachgo, S., Giblin, M.E., Taylor, D.C., and Kunst, L. (1999). *CUT1*, an Arabidopsis gene required for cuticular wax biosynthesis and pollen fertility, encodes a very-long-chain fatty acid condensing enzyme. Plant Cell **11,** 825–838.

Mitchell, A.G., and Martin, C.E. (1995). A novel cytochrome b_5-like domain is linked to the carboxyl terminus of the *Saccharomyces cerevisiae* Δ-9 fatty acid desaturase. J. Biol. Chem. **270,** 29766–29772.

Mitchell, A.G., and Martin, C.E. (1997). *Fah1p*, a *Saccharomyces cerevisiae* cytochrome b_5 fusion protein, and its *Arabidopsis thaliana* homolog that lacks the cytochrome b_5 domain both function in the α-hydroxylation of sphingolipid-associated very long chain fatty acids. J. Biol. Chem. **272,** 28281–28288.

Moose, S.P., and Sisco, P.H. (1996). *Glossy15*, an *APETALA2*-like gene from maize that regulates leaf epidermal cell identity. Genes Dev. **10,** 3018–3027.

Negruk, V., Yang, P., Subramanian, M., McNevin, J.P., and Lemieux, B. (1996). Molecular cloning and characterization of the *CER2* gene of *Arabidopsis thaliana*. Plant J. **9,** 137–145.

Niederl, S., Kirsch, T., Riederer, M., and Schreiber, L. (1998). Co-permeability of ^{3}H-labeled organic acids across isolated plant cuticles: Investigating cuticular paths of diffusion and predicting cuticular transpiration. Plant Physiol. **116,** 117–123.

Osborn, J.M., and Taylor, T.N. (1990). Morphological and ultrastructural studies of plant cuticular membranes. I. Sun and shade leaves of *Quercus velutina* (Fagaceae). Bot. Gaz. **151,** 465–476.

Pesacreta, T.C., and Hasenstein, K.H. (1999). The internal cuticle of *Cirsium horridulum* (Asteraceae) leaves. Am. J. Bot. **86,** 923–928.

Preuss, D., Lemieux, B., Yen, G., and Davis, R.W. (1993). A conditional sterile mutation eliminates surface components from *Arabidopsis* pollen and disrupts cell signaling during fertilization. Genes Dev. **7,** 974–985.

Probst, W.C., Snyder, L.A., Schuster, D.I., Brosius, J., and Sealfon, S.C. (1992). Sequence alignment of the G-protein coupled receptor superfamily. DNA Cell Biol. **11,** 1–20.

Pruitt, R.E., Vielle-Calzada, J.P., Ploense, S.E., Grossniklaus, U., and Lolle, S.J. (2000). *FIDDLEHEAD*, a gene required to suppress epidermal cell interactions in *Arabidopsis*, encodes a putative lipid biosynthetic enzyme. Proc. Natl. Acad. Sci. USA **97,** 1311–1316.

Riederer, M., and Schreiber, L. (2001). Protecting against water loss: Analysis of the barrier properties of plant cuticles. J. Exp. Bot. **52,** 2023–2032.

Schreiber, L., and Riederer, M. (1996). Ecophysiology of cuticular transpiration: Comparative investigation of cuticular water permeability of plant species from different habitats. Oecologia **107,** 426–432.

Shanklin, J., Achim, C., Schmidt, H., Fox, B.G., and Munck, E. (1997). Mossbauer studies of alkane omega-hydroxylase: Evidence for a diiron cluster in an integral-membrane enzyme. Proc. Natl. Acad. Sci. USA **94,** 2981–2986.

Shanklin, J., Whittle, E., and Fox, B.G. (1994). Eight histidine-residues are catalytically essential in a membrane-associated iron enzyme, stearoyl-CoA desaturase, and are conserved in alkane hydroxylase and xylene monooxygenase. Biochemistry **33,** 12787–12794.

Sieber, P., Schorderet, M., Ryser, U., Buchala, A., Kolattukudy, P., Metraux, J.P., and Nawrath, C. (2000). Transgenic Arabidopsis plants expressing a fungal cutinase show alterations in the structure and properties of the cuticle and postgenital organ fusions. Plant Cell **12,** 721–738.

Sperling, P., Zähringer, U., and Heinz, E. (1998). Identification of a new cytochrome b_5 fusion protein. J. Biol. Chem. **273,** 28590–28596.

Tacke, E., Korfhage, C., Michel, D., Maddaloni, M., Motto, M., Lanzini, S., Salamini, F., and Doring, H.P. (1995). Transposon tagging of the maize *Glossy2* locus with the transposable element *En*/*Spm*. Plant J. **8,** 907–917.

Thompson, J.D., Higgins, D.G., and Gibson, T.J. (1994). CLUSTAL W: The sensitivity of progressive multiple sequence alignment through sequence weighting, position-specific gap penalties and weight matrix choice. Nucleic Acids Res. **22,** 4673–4680.

Tijet, N., Helvig, C., Pinot, F., LeBouquin, R., Lesot, A., Durst, F., Salaun, J.P., and Benveniste, I. (1998). Functional expression in yeast and characterization of a clofibrate-inducible plant cytochrome P-450 (*CYP94A1*) involved in cutin monomers synthesis. Biochem. J. **332,** 583–589.

Todd, J., Post-Beittenmiller, D., and Jaworski, J.G. (1999). *KCS1* encodes a fatty acid elongase 3-ketoacyl-CoA synthase affecting wax biosynthesis in *Arabidopsis thaliana*. Plant J. **17,** 119–130.

Verbeke, J.A., and Walker, D.B. (1986). Morphogenic factors controlling differentiation and dedifferentiation of epidermal cells in the gynoecium of *Catharanthus roseus*. 2. Diffusible morphogens. Planta **168,** 43–49.

Viougeas, M.A., Rohr, R., and Chamel, A. (1995). Structural changes and permeability of ivy (*Hedera helix* L.) leaf cuticles in relation to leaf development and after selective chemical treatments. New Phytol. **130,** 337–348.

Weigel, D., et al. (2000). Activation tagging in Arabidopsis. Plant Physiol. **122,** 1003–1013.

Wellesen, K., Durst, F., Pinot, F., Benveniste, I., Nettesheim, K.,

Wisman, E., Steiner-Lange, S., Saedler, H., and Yephremov, A. (2001). Functional analysis of the *LACERATA* gene of *Arabidopsis* provides evidence for different roles of fatty acid ω-hydroxylation in development. Proc. Natl. Acad. Sci. USA **98,** 9694–9699.

Wolters-Arts, M., Lush, W.M., and Mariani, C. (1998). Lipids are required for directional pollen-tube growth. Nature **392,** 818–821.

Xia, Y., Nikolau, B.J., and Schnable, P.S. (1996). Cloning and characterization of *CER2*, an Arabidopsis gene that affects cuticular wax accumulation. Plant Cell **8,** 1291–1304.

Xu, X., Dietrich, C.R., Delledonne, M., Xia, Y., Wen, T.J., Robertson, D.S., Nikolau, B.J., and Schnable, P.S. (1997). Sequence analysis of the cloned *glossy8* gene of maize suggests that it may code for a β-ketoacyl reductase required for the biosynthesis of cuticular waxes. Plant Physiol. **115,** 501–510.

Yephremov, A., Wisman, E., Huijser, P., Huijser, C., Wellesen, K., and Saedler, H. (1999). Characterization of the *FIDDLEHEAD* gene of Arabidopsis reveals a link between adhesion response and cell differentiation in the epidermis. Plant Cell **11,** 2187–2201.

Zeiger, E., and Stebbins, G.L. (1972). Developmental genetics in barley: A mutant for stomatal development. Am. J. Bot. **59,** 143–148.

Zhao, L., and Sack, F.D. (1999). Ultrastructure of stomatal development in *Arabidopsis* (Brassicaceae) leaves. Am. J. Bot. **86,** 929–939.